A THERMAL INERTIA MAP OF TITAN AND THE EFFECTS ON A DRY CLIMATE. S. M. MacKenzie[1], R. D. Lorenz[1], J. M. Lora[2] [1]Johns Hopkins University Applied Physics Laboratory, Laurel, MD (shannon.mackenzie@jhuapl.edu), [2]Department of Geology and Geophysics, Yale University, New Haven, CT.

Introduction: Thermal inertia describes how regolith responds to thermal perturbations. This thermal response, together with albedo and topography, helps control the climate of planets with atmospheres by controlling the energy exchange between the surface and the atmosphere. This is certainly true for Titan, Saturn's largest moon, whose atmosphere resembles Earth's in composition but 4x as dense. General circulation models (GCMs) have demonstrated that employing different values for the surface thermal inertia yields changes in the surface and troposphere distributions as well as wind amplitudes [1,2]. However, these works assumed a uniform thermal inertia and *Cassini-Huygens* revealed that Titan's surface is far from homogenous.

Morphological and compositional mapping with data from Cassini-Huygens has found several classes of features. Dunes made of organic sand particles almost encircle the equatorial region [3,4,5], interrupted by the bright terrain of Xanadu replete with water-ice rich mountains [6,7]. The midlatitudes are dominated by plains materials and the enigmatic labyrinth terrain [8, 9]. At the poles, sediments—including evaporites [10]—surround the empty and liquid hydrocarbon-filled lake and sea basins [11,12]. We expect, therefore, that based on the differences in bulk composition, induration, and porosity, a map of Titan's thermal inertia would correlate with these surface units (as has been found on Mars, [e.g. 13, 14] The wealth of *Cassini* Titan observations makes a more nuanced estimate of the surface thermal properties possible.

In this work, we consolidate the available information on Titan's surface to derive a global estimate of thermal inertia and its geographical variations.

Mapping by Terrain Types: We map the surface into a 1° latitude x 1° longitude bins in equicylindrical projection (about an order of magnitude finer than the scale employed by GCMs). Cells were classified first on geomorphological expression in the RADAR dataset [15], which covers 65% of the surface. With resolutions ~ 350 m/pixel, multiple geomorphological features were sometimes within the same grid cell; we classified based on the feature that occupies the largest area within the scene. Spectral units from the Visual and Infrared Mapping Spectrometer (VIMS) [16] datasets were then correlated with RADAR units to fill in coverage gaps. VIMS has greater temporal coverage and spectral resolution, but images the surface at coarser resolutions (1-10s of km).

Given our scale of mapping and the scope of known or expected properties of Titan surface materials, we grouped all morphologies and spectral units into five terrain types: lakes (including seas), dunes, hummocky (including mountains, hills, crater rims), labyrinth, and plains. In the midlatitudes, the RADAR data can be sparse and the VIMS data coarse and poorly illuminated. Based on the correlation of the VIMS midlatitude units and RADAR plains units, these cells were classified as plains. This is likely an over estimation of plains features and perhaps an underestimate of labyrinth and hummocky terrains.

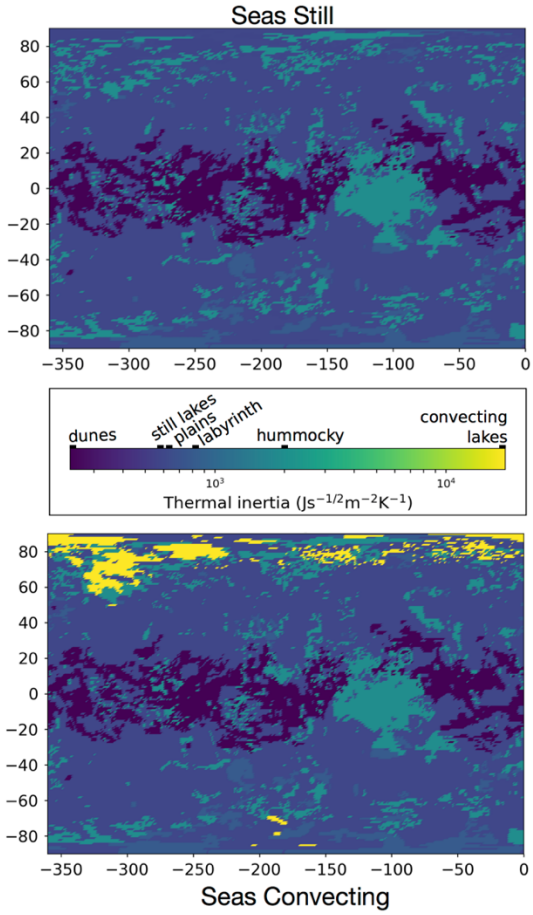

Figure 1. Thermal inertia map derived from assigning thermal conductivity, density, and specific heats to geological units based on *Cassini* data.

Thermal inertia classifications: We assigned density, thermal conductivity, and specific heat values to each terrain type based on the properties assumed from the morphologic and spectral information. For example, by analogy to terrestrial sands, we expect the porosity of Titan's dunes to be ~30% [17]. Our

estimation of sand thermal conductivity is therefore similar to [18], but we also consider the effect of the atmosphere filling the pore space as calculated from *Huygens* measurements [19]. The resulting model for Titan's sand thermal inertia (236 $Jm^{-2}s^{-1/2}K^{-1}$) is consistent with radiometric investigations of the dune fields [17, 20] and observations by *Cassini*'s Composite Infrared Spectrometer's [21].

Similar calculations were done for the other terrain types, including considering both if the lakes and seas are highly convective or minimally convective.

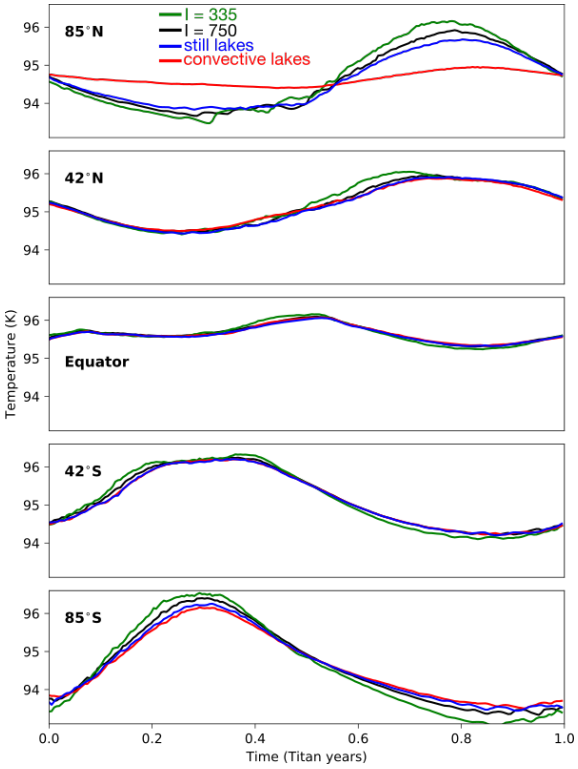

Figure 2. Surface temperature evolution at five latitudes for the four thermal inertia cases. Temperature fluctuations are most pronounced at the north pole with convective lakes where exchange between the large thermal reservoirs of the seas dampens seasonal trends.

Preliminary effects on GCM results: We use the Titan Atmospheric Model (TAM) [22] to investigate the relative effect of the thermal inertia units defined above. As the largest temperature contrasts are likely controlled by evaporation (or lack thereof) [e.g. 23], we conduct dry runs of TAM (no atmospheric moisture) to establish the minimum effect of heterogenous thermal inertia. The four test cases used (1) our thermal inertia map with minimal convection, (2) our thermal inertia map with high convection, (3) a low uniform thermal inertia [1], and (4) a higher uniform thermal inertia set to the average of our map.

In Figure 2 we show the resulting seasonal surface temperature distribution at five different latitudes. The effect of incorporating heterogenous thermal inertia is relatively minor in the models considered here. Thus, in the absence of evaporation, a single value for thermal inertia represents the thermal properties of Titan's surface well enough to be a reasonable simplification in GCMs, especially for studies focused on the equatorial region. Winds and surface temperatures track well between the four cases we considered at latitudes <40°. We expect, then, that in dry regimes where moist processes are negligible, thermal inertia does not significantly contribute to the evolution of climate; other processes must dominate. The largest differences in both surface winds and surface temperature between the four cases are found at the north pole when the lakes are deeply convective.

Future work should explore the effects of the surface thermal properties map presented here with evaporation and nonuniform methane reservoirs. Landed missions like *Dragonfly* [24,25] with instrumentation to measure the surface properties [26] at the common terrain types could be used to better constrain the global properties, as has been done with Mars remote sensing and rover mission [e.g 27].

References: [1] Tokano T. (2005) *Icarus*, 173(1), 222–242. [2] Lebonnois S. et al. (2012) *Icarus*, 218(1), 707– 722. [3] Radebaugh J. R. et al. (2008) *Icarus*, 194(2), 690–703. [4] Lorenz R. D., and J. Radebaugh (2009) *GRL*, 36, 3202 [5] Barnes J. W. et al. (2008) *Icarus*, 195(1), 400–414. [6] Barnes J. W., J. et al. (2007) JGRP, 112(E11). [7] Radebaugh J., et al. (2007) *Icarus*, 192(1), 77–91. [8] Malaska M. J., et al. (2016), *Icarus*, 270, 130–161. [9] Lopes R. M., et al. (2016) *Icarus*, 270, 162–182. [10] MacKenzie S. M. et al. (2014) *Icarus*, 243, 191–207 [11] Hayes A. et al. (2008). *GRL* 35(9). [12] Birch S. et al. (2017) *Icarus*, 282, 214–236. [13] Christensen P. R. (1983) *Icarus*, 56(3), 496–518. [14] Edgett K. S., and P. R. Christensen (1994) *JGRP*, 99(E1), 1997–2018. [15] Elachi, C. et al. (2004), The Cassini-Huygens Mission, pp. 71–110, Springer. [16] Brown R. H., et al. (2004). *Space Science Reviews*, 115(1-4), 111-168. [17] Le Gall A., M. et al. (2011), *Icarus*, 213 (2), 608–624. [18] Schurmeier L. R., and A. J. Dombard (2018) *Icarus*, 305, 314–323. [19] Hathi B., (2008), *Icarus*, 197(2), 579–584 [20] Janssen M. A. et al. (2016) Icarus, 270, 443–459. [21] Cottini V. *P&SS*, 60(1), 62–71. [22] Lora J. M. (2014) *Icarus*, 243, 264–273. [23] Mitchell J. L. (2008) *JGRP* 113, 8015 [24] Turtle E. P., et al (2019) LPSC 50 [25] Lorenz R.D. et al. (2018) *APL Tech Digest* 34, 374-387. [26] MacKenzie S. M. et al. (2019) LPSC 50 [27] Fergason R. L. (2006) *JGRP*, 111(E2)